

Supporting Information for:

**Fine-tuning side-chains of non-fullerene small molecule acceptors
to match with appropriate polymer donors**

Meijia Chang, Yunchuang Wang, Yuan-Qiu-Qiang Yi, Xin Ke, Xiangjian Wan^{*}, Chenxi
Li and Yongsheng Chen^{*}

State Key Laboratory of Elemento-Organic Chemistry, Centre of Nanoscale Science
and Technology and Key Laboratory of Functional Polymer Materials, College of
Chemistry, Nankai University, Tianjin 300071, China

*Email: xjwan@nankai.edu.cn

yschen99@nankai.edu.cn

1. Instruments and measurements

All ^1H , ^{13}C nuclear magnetic resonance spectra (NMR) were recorded in CDCl_3 on a Bruker AV400 Spectrometer. The ^1H NMR was recorded at 400MHz, ^{13}C NMR was recorded at 100MHz. All shifts were reported in ppm as downfield from TMS as standard. Multiplicity was indicated as follows: s (singlet), d (doublet), t (triplet), q (quartet), m (multiplet). Coupling constants J were reported in Hz. MALDI-TOF spectra were performed on a Bruker Autoflex III instrument. UV-Vis spectra were obtained with the JASCOV-570 spectrophotometer. The thermogravimetric analysis (TGA) was carried out on a NETZSCH STA 409 PC instrument under purified nitrogen gas flow and the heating rate and the cooling rate were $10\text{ }^\circ\text{C min}^{-1}$. Cyclic voltammetry (CV) experiments were obtained by a LK2010 electrochemical workstation. The CV measurements were taken at room temperature with three-electrode configuration, namely, a saturated calomel electrode as the reference electrode, a glassy carbon electrode as the working electrode and a Pt wire as the counter electrode. The supporting electrolyte was the solution of tetrabutylammonium phosphorus hexafluoride (Bu_4NPF_6 , 0.1 M) in dichloromethane and the scan rate was 100 mV S^{-1} .

Atomic force microscopy (AFM) was performed using Multimode 8 atomic force microscope in tapping mode. The transmission electron microscopy (TEM) investigation was performed on Philips Technical G²F20 at 200 kv. Space charge limited current (SCLC) mobility was measured using a diode configuration of ITO/PEDOT:PSS/donor:acceptor/Au for hole mobility and glass/Al/donor:acceptor/Al for electron mobility and fitting the results to space charge limited form, where SCLC equation is described by :

$$J = \frac{9\varepsilon_0\varepsilon_r\mu_0V^2}{8L^3}$$

where J is the current density, L is the film thickness of the active layer, μ_0 is the hole mobility, ε_r is the relative dielectric constant of the transport medium, ε_0 is the permittivity of free space ($8.85 \times 10^{-12}\text{ F m}^{-1}$), V is the internal voltage in the device ($= V_{\text{appl}} - V_{\text{bi}}$), where V_{appl} is the voltage applied to the device and V_{bi} is the built-in voltage due to the relative work function difference of the two electrodes.

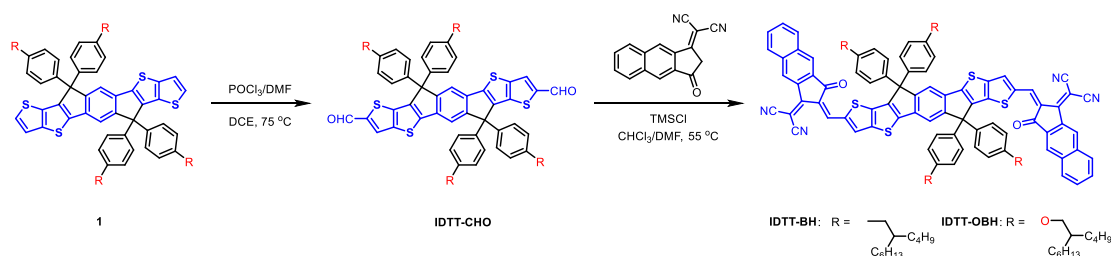
2. Organic solar cell fabrication

The devices were fabricated with a structure of glass/ITO/PEDOT:PSS/donor:acceptor/PDINO/Al. The ITO-coated glass substrates were cleaned by ultrasonic treatment in detergent, deionized water, acetone, and isopropyl alcohol under ultra-sonication for 15 minutes each and subsequently dried by a nitrogen blow. A thin layer of PEDOT:PSS (Clevios P VP AI 4083, filtered at 0.45 μm) was spin-coated at 4500 rpm onto ITO surface. After baked at 150 $^{\circ}\text{C}$ for 20 minutes, the substrates were transferred into an argon-filled glove box. Subsequently, the active layer was spin-coated from the blend chloroform solutions of donor and acceptor. Then PDINO dissolved in methanol was spin-coated. Finally, 80 nm Al layer were deposited under high vacuum ($< 2 \times 10^{-4}$ Pa). The current density-voltage (J - V) curves of photovoltaic devices were obtained with a Keithley 2400 source-measure unit. The photocurrent was measured under illumination simulated AM 1.5G (100 mW cm^{-2}) irradiation using a SAN-EI XES-70S1 solar simulator, calibrated with a standard Si solar cell. External quantum efficiencies were measured using Stanford Research Systems SR810 lock-in amplifier.

3. Synthetic route and characterization of the materials.

All reactions were carried out under argon atmosphere by using the standard Schlenk tube techniques. All starting materials were purchased from commercial sources without any purification unless stated otherwise.

Scheme S1. Synthetic route of IDTT-BH and IDTT-OBH.



Compound IDTT-BH-CHO: A Vilsmeier reagent, which was prepared with POCl₃ (2 mL, 21.5 mmol) in dry DMF (8 mL), was added to a solution of compound 1 (400 mg, 0.29 mmol) in 1,2-dichloroethane (100 mL) at 0 $^{\circ}\text{C}$ and then stirred at room temperature for 2h. After being stirred at 75 $^{\circ}\text{C}$ for 12h, the mixture was poured into ice

water (200 mL), neutralized with NaOAc, and then extracted with dichloromethane. The combined organic layer was washed with water and brine, dried over Na₂SO₄. After removal of solvent it was chromatographed on silica gel using a mixture of dichloromethane and petroleum ether as eluant to afford **IDTT-BH-CHO** as a yellow solid (354 mg, 85% yield).

¹H NMR (400 MHz, CDCl₃) δ 9.88 (s, 2H), 7.94 (s, 2H), 7.63 (s, 2H), 7.14 (d, J = 8.1 Hz, 8H), 7.06 (d, J = 8.2 Hz, 8H), 2.48 (d, J = 6.9 Hz, 8H), 1.58 – 1.55 (m, 4H), 1.27 – 1.17 (m, 64H), 0.88 – 0.80 (m, 24H).

¹³C NMR (101 MHz, CDCl₃) δ 182.82, 154.66, 149.48, 146.74, 144.41, 141.72, 141.32, 140.27, 139.16, 136.51, 129.54, 127.68, 118.02, 63.17, 40.21, 39.41, 33.30, 32.90, 31.87, 29.62, 28.78, 26.52, 22.97, 22.66, 14.13, 14.09.

MS (MALDI-TOF): calcd. for C₉₄H₁₂₂O₂S₄ [M⁺] 1411.8361, found 1412.5795.

Compound IDTT-OBH-CHO: the same procedure was used as for **IDTT-BH-CHO**. Yield: 346 mg (81%).

¹H NMR (400 MHz, CDCl₃) δ 9.89 (s, 2H), 7.94 (s, 2H), 7.57 (s, 2H), 7.15 (d, J = 8.8 Hz, 8H), 6.81 (d, J = 8.8 Hz, 8H), 3.77 (d, J = 5.5 Hz, 8H), 1.77 – 1.68 (m, 4H), 1.37 – 1.23 (m, 64H), 0.91 – 0.82 (m, 24H).

¹³C NMR (101 MHz, CDCl₃) δ 182.81, 158.79, 155.02, 149.24, 147.04, 144.42, 141.82, 140.05, 136.37, 133.63, 129.86, 128.98, 117.80, 114.60, 70.76, 62.37, 37.94, 31.84, 31.36, 31.05, 29.67, 29.06, 26.82, 23.04, 22.67, 14.10, 14.08.

MS (MALDI-TOF): calcd. for C₉₄H₁₂₂O₆S₄ [M⁺] 1475.8158, found 1475.9914.

Compound IDTT-BH: compound IDTT-BH-CHO (100 mg, 0.071 mmol) and NINCN (138 mg, 0.57 mmol) were dissolved in dry CHCl₃ (35 mL) and then TMSCl (2 mL) and DMF (5 mL) were added. Under the protection of argon, the mixture was stirred for 24h at 75 °C. After removal of solvent, the crude product was purified by silica gel using chloroform as eluent to afford **IDTT-BH** as dark green solid. (90 mg, 68% yield).

¹H NMR (400 MHz, CDCl₃) δ 9.16 (s, 2H), 8.91 (s, 2H), 8.36 (s, 2H), 8.24 (s, 2H), 8.06 – 7.98 (m, 4H), 7.66 (d, J = 7.7 Hz, 6H), 7.24 (d, J = 8.3 Hz, 8H), 7.13 (d, J = 8.3 Hz, 8H), 2.50 (d, J = 6.6 Hz, 8H), 1.63 – 1.57 (m, 4H), 1.28 – 1.18 (m, 64H), 0.87 – 0.77 (m, 24H).

^{13}C NMR (101 MHz, CDCl_3) δ 187.96, 160.32, 155.94, 153.36, 147.97, 147.71, 143.94, 141.56, 140.24, 138.87, 138.58, 137.10, 136.31, 135.46, 134.78, 132.93, 130.67, 130.20, 129.89, 129.75, 129.64, 127.77, 126.93, 124.71, 124.60, 118.65, 115.24, 115.05, 68.13, 63.39, 40.26, 39.43, 33.39, 33.35, 32.99, 32.94, 31.89, 29.65, 28.85, 28.81, 26.58, 26.55, 23.00, 22.67, 14.11.

MS (MALDI-TOF): calcd. for $\text{C}_{126}\text{H}_{134}\text{N}_4\text{O}_2\text{S}_4$ [M+] 1863.9423, found 1864.9310.

Compound IDTT-OBH: the same procedure was used as for **IDTT-BH**. Yield: 102 mg (75%).

^1H NMR (400 MHz, CDCl_3) δ 9.18 (s, 2H), 8.94 (s, 2H), 8.38 (s, 2H), 8.24 (s, 2H), 8.09 – 8.01 (m, 4H), 7.72 – 7.67 (m, 4H), 7.62 (s, 2H), 7.24 (d, $J = 9.0$ Hz, 8H), 6.87 (d, $J = 8.8$ Hz, 8H), 3.79 (d, $J = 5.5$ Hz, 8H), 1.77 – 1.69 (m, 4H), 1.36 – 1.21 (m, 64H), 0.89 – 0.82 (m, 24H).

^{13}C NMR (101 MHz, CDCl_3) δ 188.08, 160.35, 159.03, 156.28, 153.13, 148.30, 147.49, 143.99, 140.24, 138.64, 137.25, 137.00, 136.33, 135.47, 134.80, 133.36, 132.94, 130.68, 130.23, 129.92, 129.68, 129.09, 126.95, 124.65, 118.46, 115.06, 114.85, 70.89, 68.19, 62.57, 38.03, 31.85, 31.44, 31.12, 29.68, 29.11, 26.87, 23.05, 22.67, 14.08.

MS (MALDI-TOF): calcd. for $\text{C}_{126}\text{H}_{134}\text{N}_4\text{O}_6\text{S}_4$ [M+] 1927.9220, found 1928.9868.

4. Thermogravimetric analysis of IDTT-BH and IDTT-OBH.

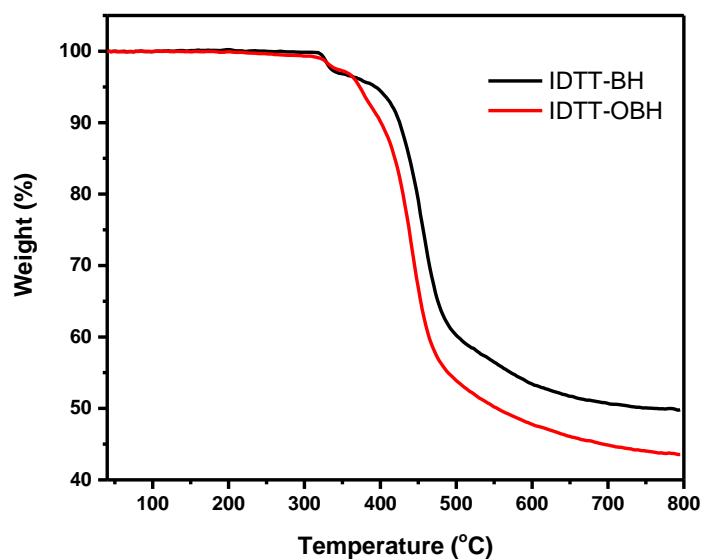


Figure S1. Thermogravimetric analysis (TGA) plot of IDTT-BH and IDTT-OBH.

5. Cyclic voltammogram of IDTT-BH and IDTT-OBH.

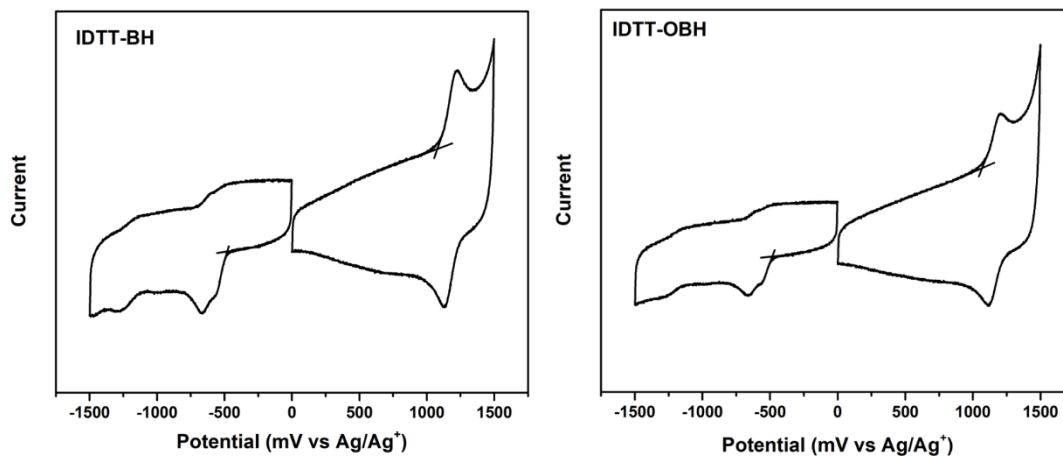


Figure S2. Cyclic voltammogram of IDTT-BH and IDTT-OBH in dichloromethane solution.

6. The optimized device conditions of J71:IDTT-BH and J71:IDTT-OBH system.

Table S1. Photovoltaic performance of BHJ solar cells based on **J71:IDTT-BH** with donor concentration (5 mg/mL) and under illumination of AM 1.5 G 100 mW cm⁻². The active layer was casted from CHCl₃ solution with different weight ratios. PDINO/Al was used as the cathode.

ratios	V _{oc} (V)	J _{sc} (mA cm ⁻²)	FF (%)	PCE (%)
1:1	0.89	13.01	64.1	7.41
1:1.2	0.89	14.07	63.6	7.96
1:1.4	0.89	14.81	63.1	8.31
1:1.6	0.88	15.49	59.3	8.17
1:1.8	0.87	16.70	55.3	8.08

Table S2. Photovoltaic performance of BHJ solar cells based on **J71:IDTT-BH** with donor concentration (5 mg/mL) and under illumination of AM 1.5 G 100 mW cm⁻². The weight ratio of donor and acceptor is 1:1.4. The active layer was casted from CHCl₃ solution with different SVA times. PDINO/Al was used as the cathode.

times	V _{oc} (V)	J _{sc} (mA cm ⁻²)	FF (%)	PCE (%)
0s	0.89	14.81	63.1	8.31
60s	0.89	16.12	65.3	9.39
90s	0.89	17.05	66.9	10.15
120s	0.90	17.77	69.1	11.05
150s	0.89	16.61	65.3	9.71

Table S3. Photovoltaic performance of BHJ solar cells based on **J71:IDTT-OBH** with donor concentration (5 mg/mL) and under illumination of AM 1.5 G 100 mW cm⁻². The active layer was casted from CHCl₃ solution with different weight ratios. PDINO/Al was used as the cathode.

Ratios	V _{oc} (V)	J _{sc} (mA cm ⁻²)	FF (%)	PCE (%)
1:0.8	0.93	11.46	58.7	6.28
1:1	0.93	12.12	58.6	6.61
1:1.2	0.93	12.21	55.8	6.37
1:1.4	0.93	13.13	51.6	6.28

Table S4. Photovoltaic performance of BHJ solar cells based on **J71:IDTT-BH** with donor concentration (5 mg/mL) and under illumination of AM 1.5 G 100 mW cm⁻². The weight ratio of donor and acceptor is 1:1. The active layer was casted from CHCl₃ solution with different SVA times. PDINO/Al was used as the cathode.

Times (s)	V_{oc} (V)	J_{sc} (mA cm ⁻²)	FF (%)	PCE (%)
80	0.93	13.19	57.8	7.08
100	0.92	13.61	57.7	7.24
120	0.92	14.75	61.0	8.02
140	0.90	14.85	49.7	6.24

7. The optimized device conditions of PDCBT:IDTT-BH and PDCBT:IDTT-OBH system.

Table S5. Photovoltaic performance of BHJ solar cells based on **PDCBT:IDTT-BH** with donor concentration (5 mg/mL) and under illumination of AM 1.5 G 100 mW cm⁻². The weight ratio of donor:acceptor was 1:1. The active layer was casted from CHCl₃ solution with different TA temperature. PDINO/Al was used as the cathode.

Temperature (°C)	V_{oc} (V)	J_{sc} (mA cm ⁻²)	FF (%)	PCE (%)
80	0.90	10.71	64.9	6.24
100	0.89	13.01	64.1	7.41
120	0.87	16.93	67.5	9.96
140	0.85	17.25	64.8	9.50
160	0.83	16.67	58.1	8.04

Table S6. Photovoltaic performance of BHJ solar cells based on **PDCBT:IDTT-BH** with donor concentration (5 mg/mL) and under illumination of AM 1.5 G 100 mW cm⁻². The TA temperature was 120 °C. The active layer was casted from CHCl₃ solution with different weight ratios. PDINO/Al was used as the cathode.

Ratios	V_{oc} (V)	J_{sc} (mA cm ⁻²)	FF (%)	PCE (%)
1:0.8	0.87	15.36	68.0	9.08
1:1	0.87	16.93	67.5	9.96
1:1.2	0.88	17.15	68.6	10.35
1:1.4	0.87	16.84	67.4	9.87

Table S7. Photovoltaic performance of BHJ solar cells based on **PDCBT:IDTT-OBH** with donor concentration (5 mg/mL) and under illumination of AM 1.5 G 100 mW cm⁻². The active layer was casted from CHCl₃ solution with different weight ratios. PDINO/Al was used as the cathode.

Ratios	V_{oc} (V)	J_{sc} (mA cm ⁻²)	FF (%)	PCE (%)
1:0.8	0.92	11.15	50.0	5.14
1:1	0.94	11.47	59.3	6.39
1:1.2	0.94	12.32	57.8	6.69
1:1.4	0.94	12.09	50.9	5.76

Table S8. Photovoltaic performance of BHJ solar cells based on **PDCBT:IDTT-OBH** with donor concentration (5 mg/mL) and under illumination of AM 1.5 G 100 mW cm⁻². The weight ratio of donor:acceptor was 1:1.2. The active layer was casted from CHCl₃ solution with different TA temperature. PDINO/Al was used as the cathode.

Temperature (°C)	V_{oc} (V)	J_{sc} (mA cm ⁻²)	FF (%)	PCE (%)
none	0.94	12.32	57.8	6.69
100	0.92	13.57	62.9	7.85
120	0.91	13.97	64.8	8.24
140	0.91	13.25	63.6	7.67
160	0.91	13.06	62.9	7.48

8. The optimized device conditions of PBDB-T:IDTT-BH and PBDB-T:IDTT-OBH system.

Table S9. Photovoltaic performance of BHJ solar cells based on **PBDB-T:IDTT-BH** with donor concentration (5 mg/mL) and under illumination of AM 1.5 G 100 mW cm⁻². The active layer was casted from CHCl₃ solution with different weight ratios. PDINO/Al was used as the cathode.

Ratios	V_{oc} (V)	J_{sc} (mA cm ⁻²)	FF (%)	PCE (%)
1:0.6	0.85	13.76	69.5	8.13
1:0.8	0.87	15.25	70.5	9.33
1:1	0.87	15.35	68.3	9.12
1:1.2	0.87	15.90	65.2	9.02
1:1.4	0.87	15.18	64.4	8.52

Table S10. Photovoltaic performance of BHJ solar cells based on **PBDB-T:IDTT-BH** with donor concentration (5 mg/mL) and under illumination of AM 1.5 G 100 mW cm⁻². The weight ratio of donor:acceptor was 1:0.8. The active layer was casted from CHCl₃ solution with different TA temperature. PDINO/Al was used as the cathode.

Temperature (°C)	V _{oc} (V)	J _{sc} (mA cm ⁻²)	FF (%)	PCE (%)
None	0.87	15.25	70.5	9.33
80	0.86	16.31	68.8	9.52
100	0.85	16.86	69.2	9.92
120	0.85	15.15	67.0	8.66

Table S11. Photovoltaic performance of BHJ solar cells based on **PBDB-T:IDTT-OBH** with donor concentration (5 mg/mL) and under illumination of AM 1.5 G 100 mW cm⁻². The active layer was casted from CHCl₃ solution with different weight ratios. PDINO/Al was used as the cathode.

Ratios	V _{oc} (V)	J _{sc} (mA cm ⁻²)	FF (%)	PCE (%)
1:0.6	0.86	13.37	68.5	7.88
1:0.8	0.87	15.70	70.3	9.60
1:1	0.87	15.37	69.0	9.30
1:1.2	0.88	15.52	67.3	9.19
1:1.4	0.88	15.29	66.9	9.00

Table S12. Photovoltaic performance of BHJ solar cells based on **PBDB-T:IDTT-OBH** with donor concentration (5 mg/mL) and under illumination of AM 1.5 G 100 mW cm⁻². The weight ratio of donor:acceptor was 1:0.8. The active layer was casted from CHCl₃ solution with different TA temperature. PDINO/Al was used as the cathode.

Temperature (°C)	V _{oc} (V)	J _{sc} (mA cm ⁻²)	FF (%)	PCE (%)
None	0.87	15.70	70.3	9.60
90	0.86	16.60	70.7	10.09
110	0.87	17.46	72.0	10.93
130	0.87	16.99	69.9	10.33
150	0.87	16.76	68.2	9.97

9. NMR spectra.

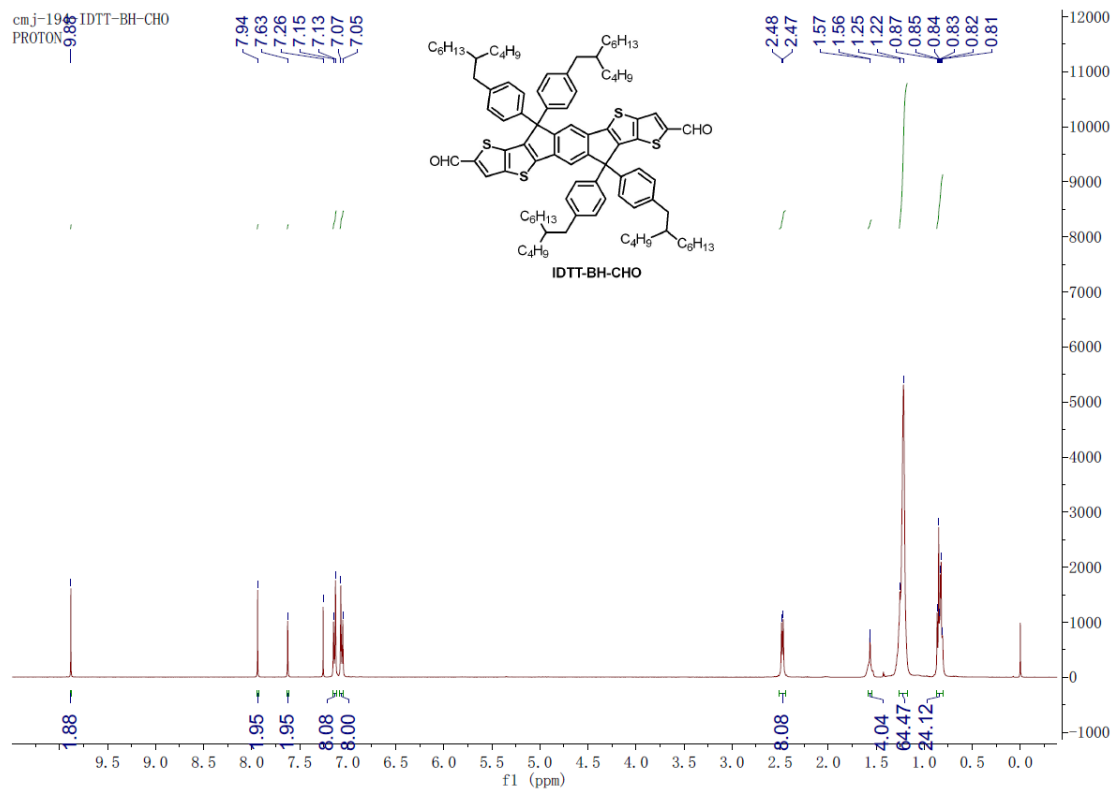


Figure S3. ¹H NMR spectra of IDTT-BH-CHO at 300K in CDCl₃.

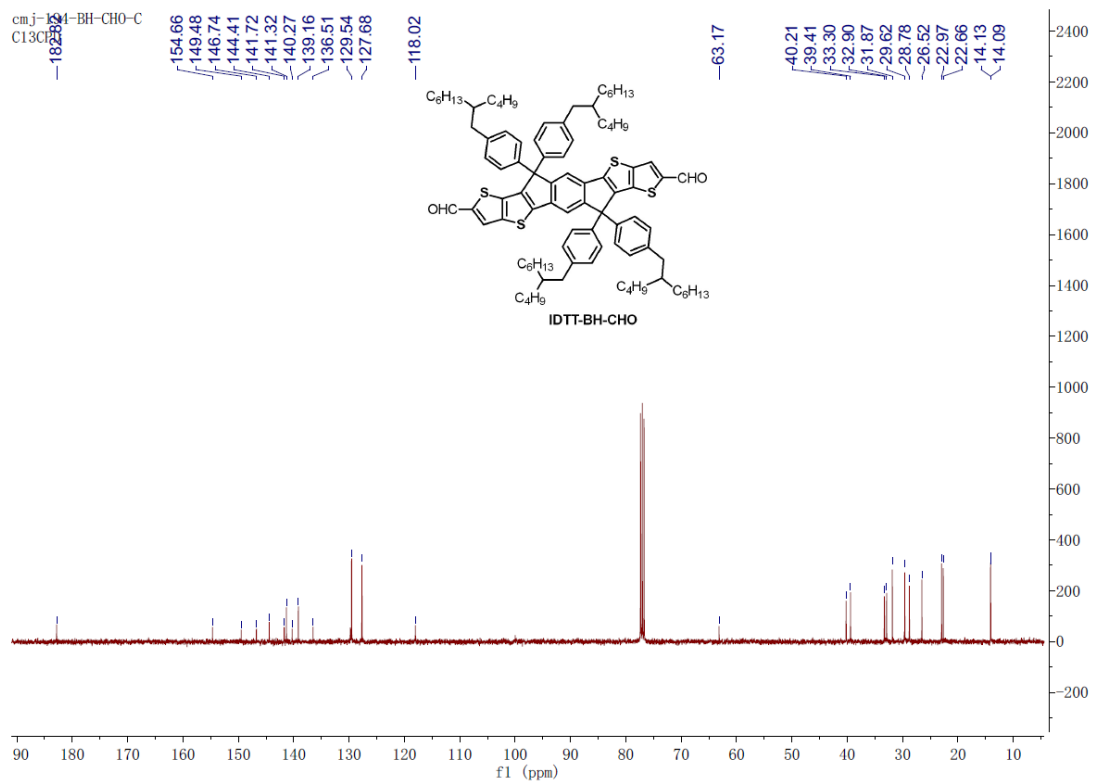


Figure S4. ¹³C NMR spectra of IDTT-BH-CHO at 300K in CDCl₃.

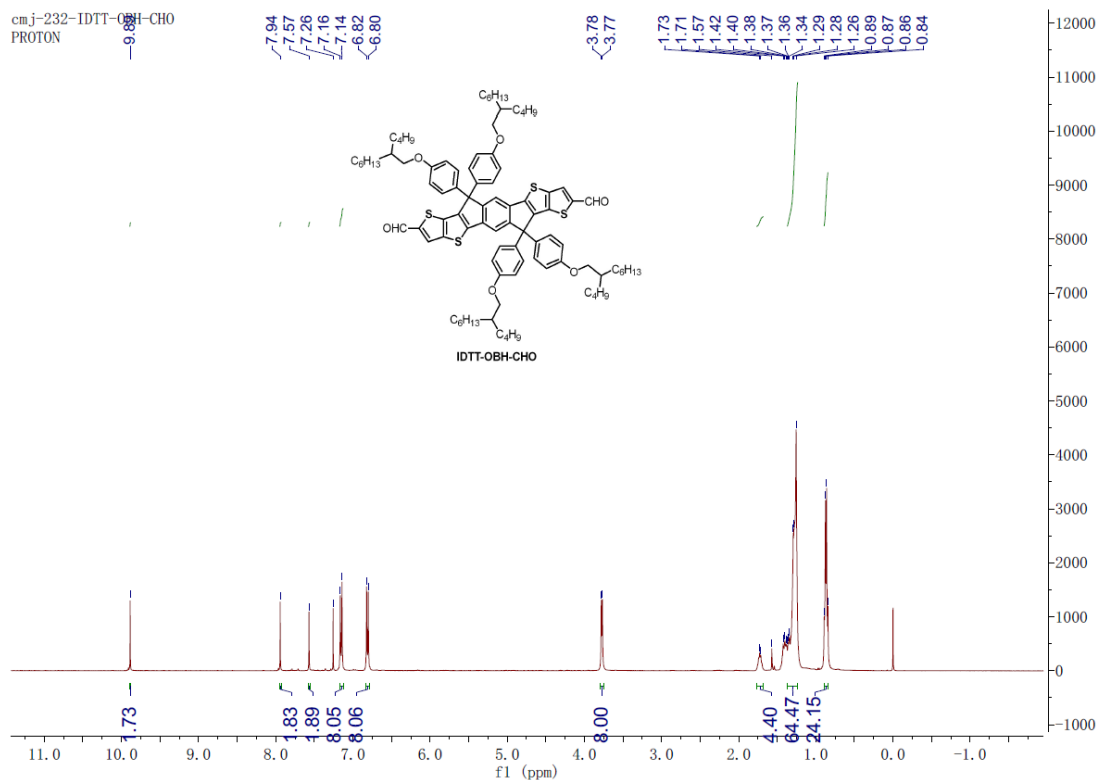


Figure S5. ^1H NMR spectra of IDTT-OBH-CHO at 300K in CDCl_3 .

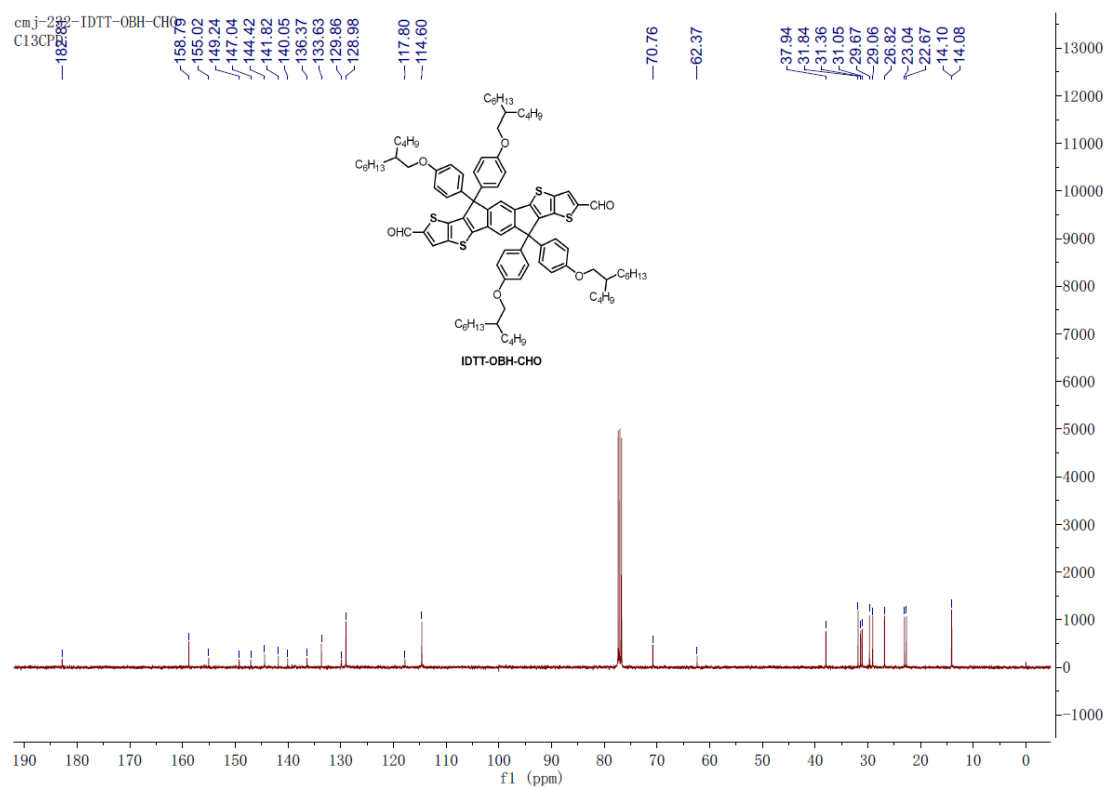


Figure S6. ^{13}C NMR spectra of IDTT-OBH-CHO at 300K in CDCl_3 .

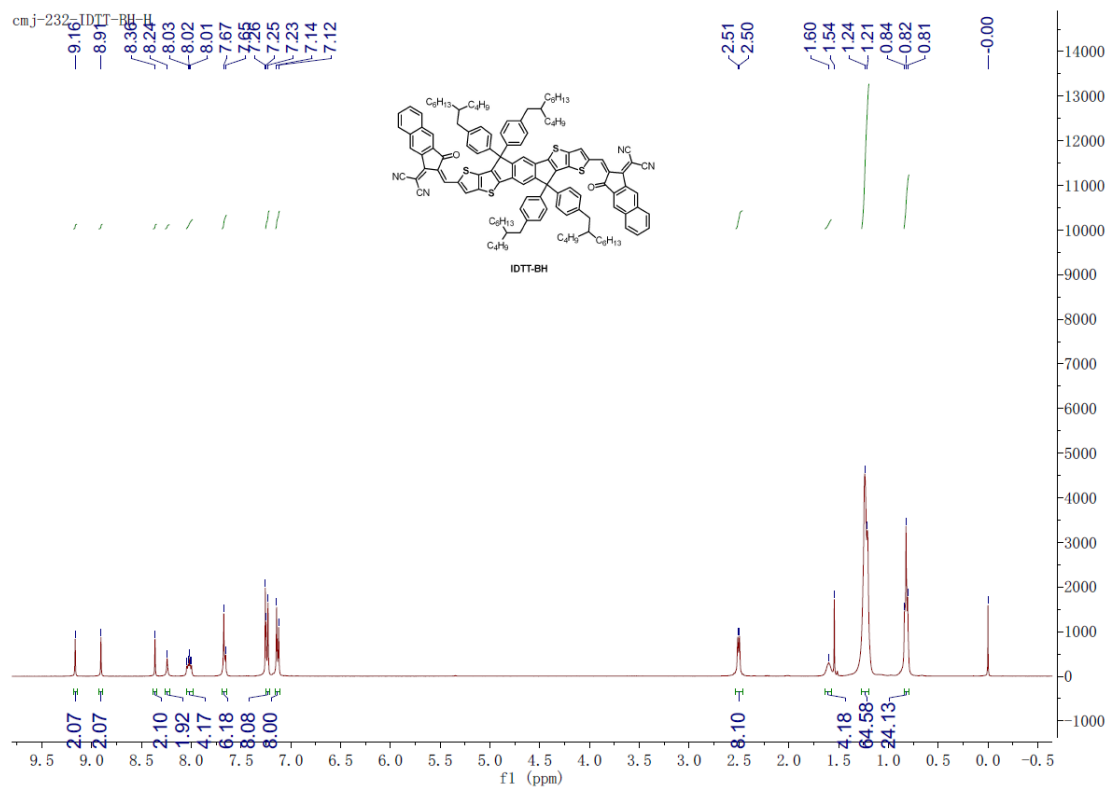


Figure S7. ^1H NMR spectra of **IDTT-BH** at 300K in CDCl_3 .

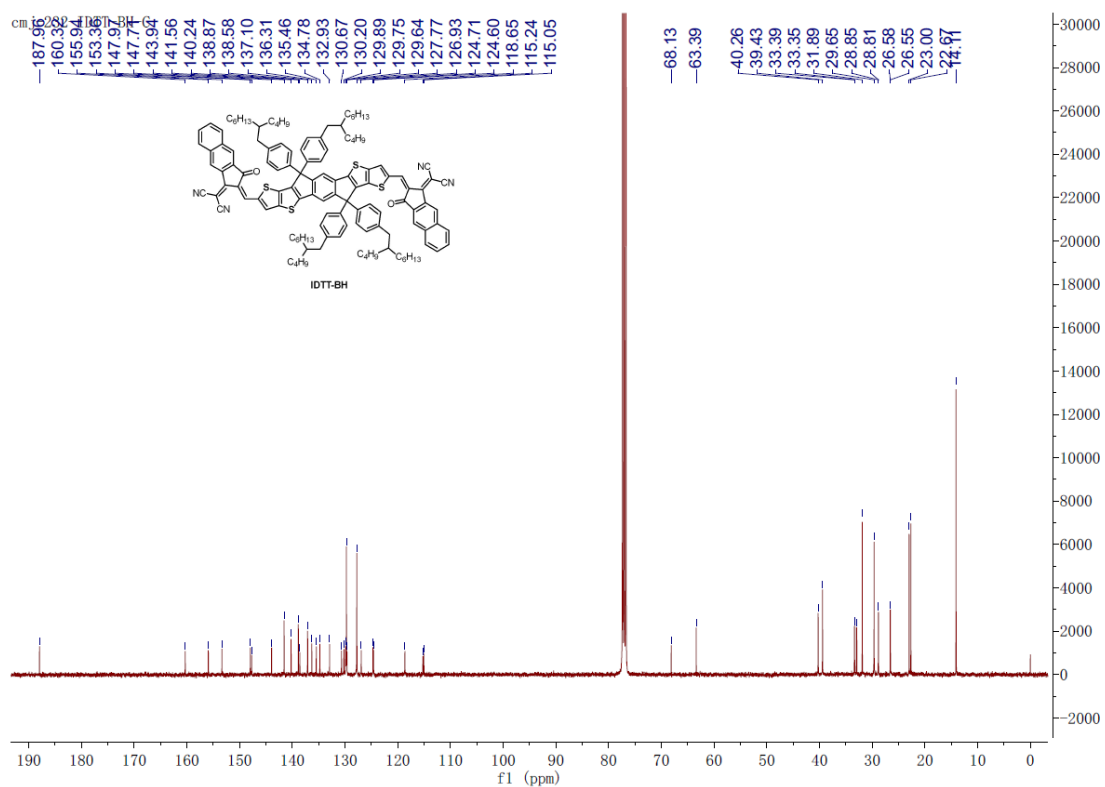


Figure S8. ^{13}C NMR spectra of **IDTT-BH** at 300K in CDCl_3 .

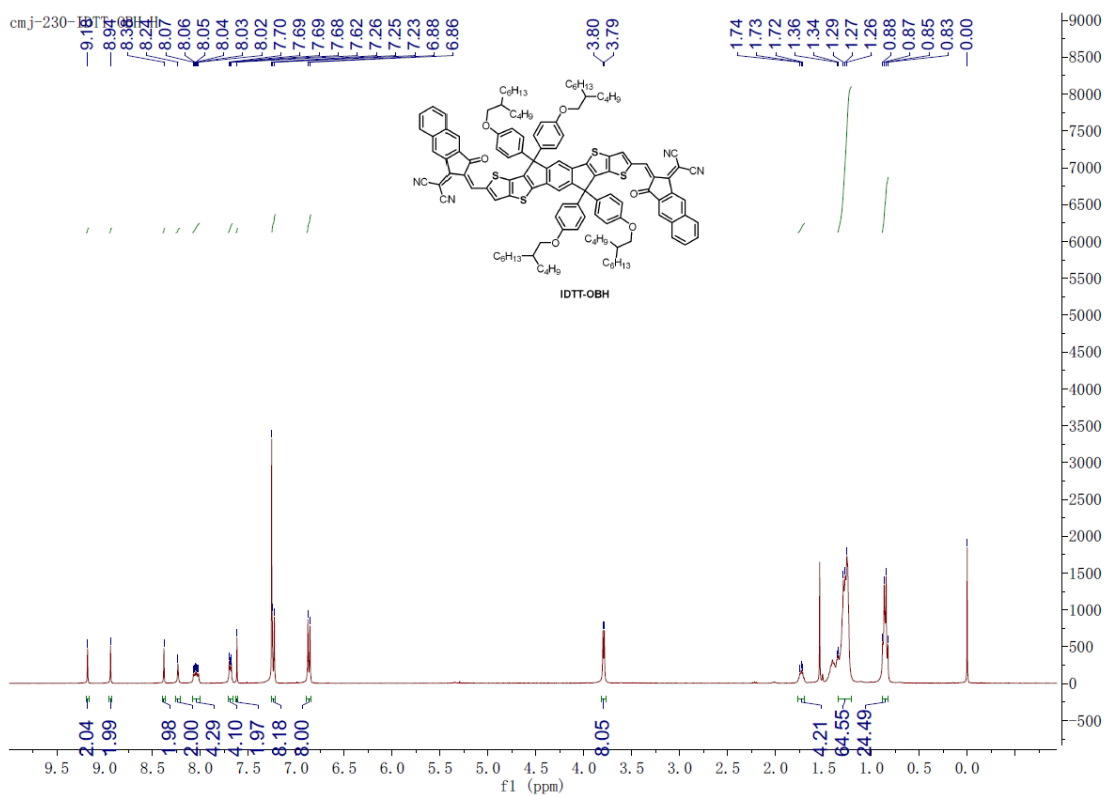


Figure S9. ¹H NMR spectra of IDTT-OBH at 300K in CDCl₃.

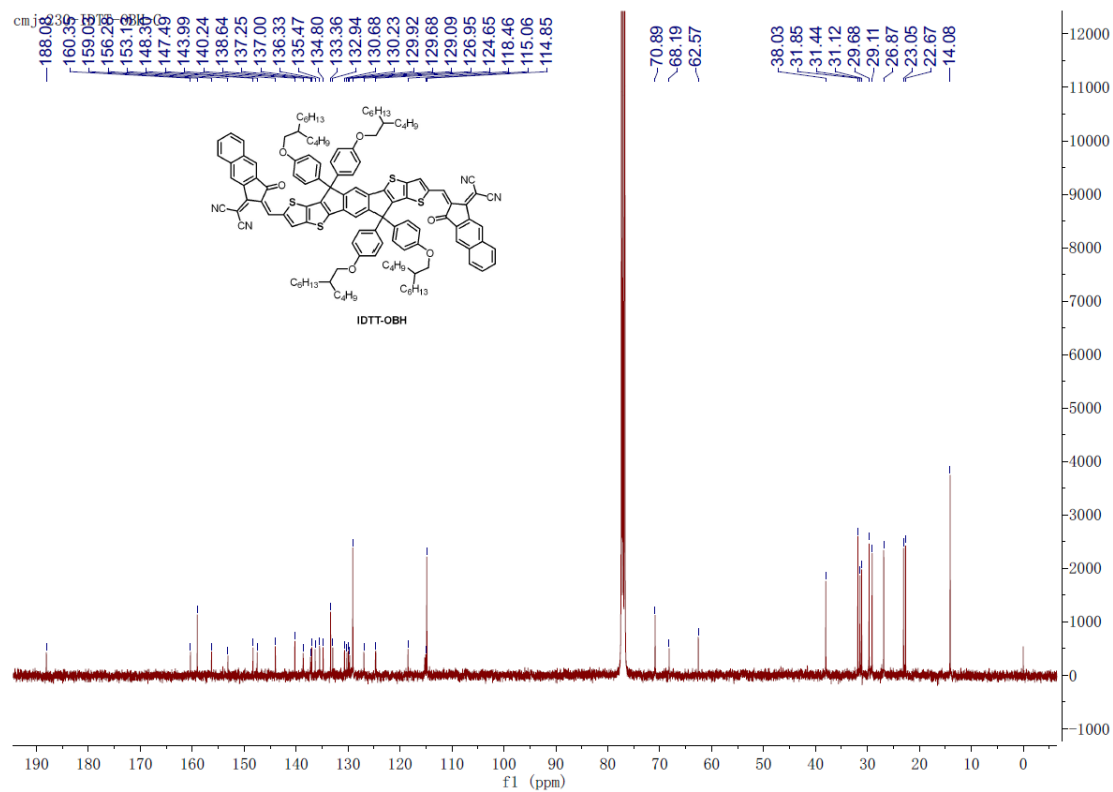


Figure S10. ¹³C NMR spectra of IDTT-OBH at 300K in CDCl₃.

10. 2D-GIXD patterns for blending films.

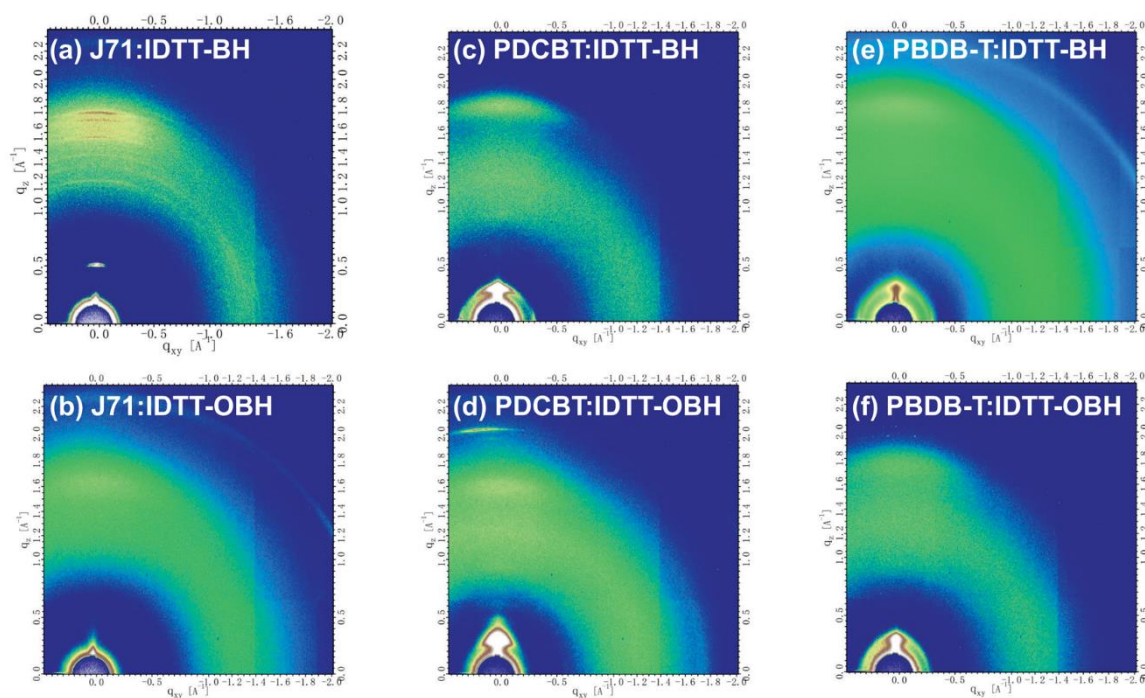


Figure S11. 2D-GIXD patterns for blending films of **J71:IDTT-BH/IDTT-OBH** (a/b), **PDCBT:IDTT-BH/IDTT-OBH** (c/d) and **PDCBT:IDTT-BH/IDTT-OBH** (e/f).

11. Optimized molecular geometries.

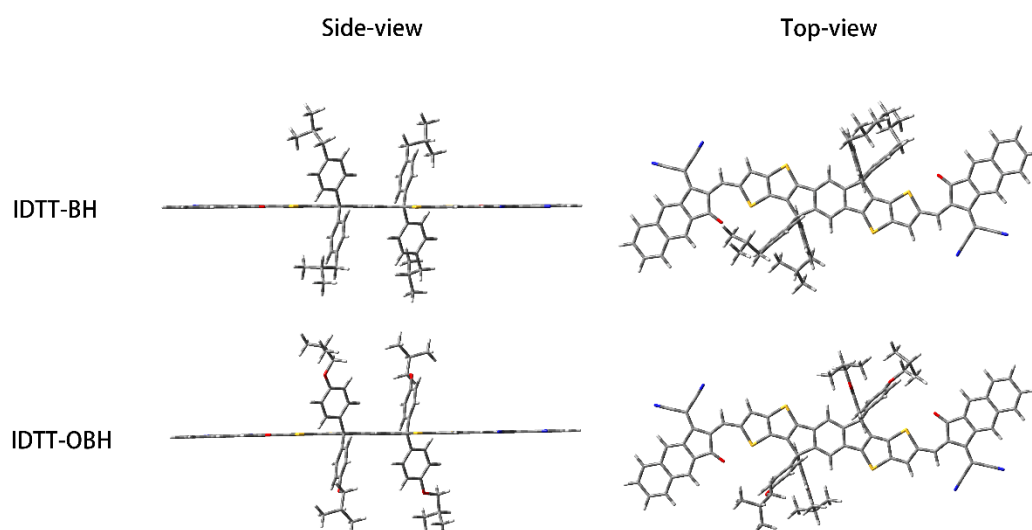


Figure S12. Optimized molecular geometries of **IDTT-BH** and **IDTT-OBH**.